



Thermal pasteurization process evaluation using mashed potato model food with Maillard reaction products



Ellen R. Bornhorst, Juming Tang*, Shyam S. Sablani, Gustavo V. Barbosa-Cánovas

Department of Biological Systems Engineering, Washington State University, Pullman, WA 99164-6120, USA

ARTICLE INFO

Article history:

Received 14 September 2016

Received in revised form

7 April 2017

Accepted 7 April 2017

Available online 12 April 2017

Keywords:

Quality

Kinetics

Chemical marker

Microwave-assisted pasteurization

ABSTRACT

Model foods with Maillard reaction product formation have been utilized to evaluate thermal sterilization processes, but these models are not optimal for pasteurization. Model foods for pasteurization applications have been developed, but studies on temperature sensitivity and validation are limited. The goal of this research was to assess the temperature sensitivity of chemical marker and color formation in mashed potato model foods and conduct validation testing using a microwave-assisted pasteurization system (MAPS) and conventional, hot water methods. Reaction kinetics were determined for chemical marker M-2 (4-hydroxy-5-methyl-3(2H)-furanone) and color formation (L^* and a^* values). Results showed that the thermal resistance constants (z -values) were 20.6–24.0 °C for M-2, 20.8–28.8 °C for L^* value, and 10.3–25.6 °C for a^* value. Correlation analysis between M-2, L^* , and a^* values and thermal lethality and cook value showed that model foods were most relevant for pasteurization process quality evaluation. Thermal treatment equivalent at the cold spot was approximately 11 min at 90 °C for all pasteurization processes. Model foods pasteurized in MAPS had less color change than those from hot water processes, implying the less severe MAPS process yielded better quality. Model foods and image analysis techniques used in this study could be helpful quality evaluation tools for pasteurization processes.

© 2017 Elsevier Ltd. All rights reserved.

1. Introduction

The Maillard reaction is a type of nonenzymatic browning that occurs between free amino groups and carbonyl compounds (Fayle & Gerrard, 2002). The concentration of generated Maillard reaction products are time and temperature sensitive and can be related to a time-temperature history (Van Loey, Hendrickx, De Cordt, Haentjens, & Tobback, 1996). Maillard reaction products have been used as time-temperature integrators and are an effective alternative method to measure temperature distribution inside a food package and quantify process lethality (Kim, Taub, Choi, & Prakash, 1996; Ramaswamy, Awuah, Kim, & Choi, 1996; Ross, 1993; Wang, Lau, Tang, & Mao, 2004; Wnorowski & Yaylayan, 2002). The use of time-temperature integrators as an alternative method to measure temperature distribution in food products is essential for developing thermal processes using novel technologies (e.g. ohmic heating and microwave heating), where conventional process development and temperature measurement

techniques are difficult (Kim et al., 1996).

Chemical marker M-2 (4-hydroxy-5-methyl-3(2H)-furanone) was identified as a relevant Maillard reaction product for evaluating high temperature, short time processes, such as microwave heating (Lau et al., 2003; Pandit, Tang, Mikhaylenko, & Liu, 2006). M-2 is formed as a result of 2,3 enolization of the Amadori compound during the Maillard reaction between D-ribose and an amine (Kim et al., 1996). Products generated from 2,3 enolization are similar to those from sugar degradation without amines, i.e. caramelization, but generation occurs at a different rate because amine and amino acid compounds catalyze sugar degradation during the Maillard reaction (BeMiller & Huber, 2008). M-2 and brown color formation were used conjunctly with model foods and a computer vision system to visualize the heating pattern and validate a microwave-assisted thermal sterilization (MATS) process (Pandit, Tang, Liu, & Pitts, 2007b; Tang, 2015). Homogenous model foods were employed rather than real foods because conducting these experiments with real foods can lead to inaccurate heating pattern results due to their non-homogeneity (Wang et al., 2004). Additionally, the concentration of reactants added to the model food (reducing sugar, amino acid) can be adjusted to change the reaction

* Corresponding author.

E-mail address: jtang@wsu.edu (J. Tang).

rate of the time-temperature integrators to better match food safety or quality attributes of interest. This validation technique could be employed to validate other thermal processes, such as a Microwave Assisted Pasteurization System (MAPS) that has been recently developed at Washington State University (Tang, 2015).

The patent-pending MAPS design is similar to the MATS set-up without overpressure, as described in Tang (2015). The MAPS design combines traditional hot water heating with microwave heating using 915 MHz microwaves. Microwaves (915 MHz) generated from a magnetron interact with trays of food products in single-mode cavities (Tang, 2015). Briefly, the pilot-scale MAPS set-up includes four sections: preheating, microwave heating, holding, and cooling. This system is able to process 8–20 oz (226.8–567.0 g) trays; belt speed and water temperature are commonly changed to adjust the thermal process severity delivered to the food product. Various food products have been pasteurized with the pilot-scale MAPS and the promising results from these initial tests implied the MAPS can produce safe, high quality food products. Currently, commercial-scale Microwave Assisted Pasteurization Systems for food processing are not available yet to the industry and commercialization is in progress.

The United States Food and Drug Administration (FDA, 2011) and European Chilled Food Federation (ECFF) (2006) have recommended an equivalent heat treatment of 90 °C for 10 min to achieve at least a 6 log reduction in non-proteolytic *Clostridium botulinum* spores (e.g. types B and E) for thermal pasteurization of pre-packaged, chilled food. Less severe treatments are also acceptable in food products with shorter shelf-lives, such as an equivalent heat treatment of 70 °C for 2 min for at least a 6 log reduction in *Listeria monocytogenes* (FDA, 2011; ECFF, 2006). In this study, non-proteolytic *C. botulinum* was the pathogen of interest; MAPS and hot water pasteurization processes were designed to meet the 90 °C for 10 min criteria.

Model food systems with Maillard reaction products developed for sterilization (110–130 °C) applications (Lau et al., 2003; Pandit et al., 2006; Ramaswamy et al., 1996; Ross, 1993; Wang et al., 2009) are not ideal for pasteurization (70–100 °C) applications, especially due to the slower reaction kinetics at the lower temperatures used in pasteurization. Several model foods with Maillard reaction products have been developed for pasteurization applications, including egg white model food (Bornhorst, Tang, Sablani, & Barbosa-Cánovas, 2017; Zhang, Tang, Liu, Bohnet, & Tang, 2014), gellan model food (Bornhorst et al., 2017; Zhang et al., 2015), and mashed potato model food (Bornhorst et al., 2017). Bornhorst et al. (2017) compared the performance and reaction kinetics at 90 °C for all three model foods: egg white, gellan, and mashed potato. They concluded that the optimal model food for future research was mashed potato, which is why this study utilized mashed potato model food.

Previous work by Bornhorst et al. (2017) on mashed potato model food for pasteurization applications determined the chemical marker (M-2) and brown color formation kinetics at only one temperature (90 °C). The temperature sensitivity in the pasteurization temperature range of the chemical marker and brown color formation in the mashed potato model is unknown. This missing information is critical in order to utilize the model food systems to compare pasteurization processes with various processing temperatures and differing time-temperature histories. Additionally, previous research on model foods for pasteurization was focused on formula development and reaction kinetic studies with very limited work on validation of the models in food processing applications. Therefore, the objectives of this research were to (1) Determine the temperature dependence of M-2 and color formation in the mashed potato model food and (2) Perform a validation by pasteurizing the mashed potato model food using MAPS and hot

water methods.

2. Materials and methods

2.1. Sample preparation

The model food (100 g) was prepared with 15 g instant mashed potato flakes (Oregon Potato Co. Boardman, OR), 0.5 g low acyl gellan gum (Kelcogel® F Food grade gellan gum, supplied by CP Kelco Inc. Atlanta, GA), 0.13 g calcium chloride ($\text{CaCl}_2 \cdot 2\text{H}_2\text{O}$, J.T. Baker, Avantor Performance Materials, Inc. Center Valley, PA), 1–2 g D-ribose (Sigma-Aldrich Co. LLC, St. Louis, MO), 0.5–2 g L-lysine (Sigma-Aldrich Co. LLC, St. Louis, MO), and deionized and distilled water (80.37–84.37 g), as described in Bornhorst et al. (2017). Different quantities of D-ribose and L-lysine, the chemical marker precursors, were added to alter the reaction rates. The models used in this study included 1 g/100 g D-ribose and 0.5 g/100 g L-lysine, 1 g/100 g D-ribose and 1 g/100 g L-lysine, and 2 g/100 g D-ribose and 2 g/100 g L-lysine, abbreviated in the paper as 1_R, 0.5_L, 1_R, 1_L, and 2_R, 2_L. Calcium chloride was added to the model food systems in order to facilitate the gel setting to form a strong, brittle, and heat stable gel (Morris, Nishinari, & Rinaudo, 2012; Tang, Tung, & Zeng, 1996, Tang, Tung, & Zeng, 1997). Calcium chloride also affects the rate of Maillard browning (Kocadağlı & Gökmen, 2016); for this reason, the amount calcium chloride added to each formula was kept constant to maintain consistency.

The preparation protocol for the mashed potato model foods was adapted from Bornhorst et al. (2017). Briefly, gellan gum and mashed potato flakes were mixed with deionized and distilled water and heated to 90 °C, followed by the addition of calcium chloride and holding at 90 °C for 1 min. The mixture was cooled to 60 °C and D-ribose and L-lysine were thoroughly mixed into the model food. A firm gel was formed upon cooling to ambient conditions (22 °C).

2.2. Temperature kinetic study

Mashed potato model foods were exposed to heat, followed by chemical marker (M-2) and color quantification. Model foods were heated inside 1 mL cylindrical, aluminum test cells (Chung, Birla, & Tang, 2008) with a water bath (80 °C) and ethylene glycol bath (100 °C) (HAAKE DC 30, Thermo Fisher Scientific Inc. Newington, NH) and cooled in ice water (0 °C). The time for the coldest spot in the kinetic cell to reach within 0.5 °C of the set point temperature (come-up time, CUT) was 1.75 min, as measured by calibrated type-T thermocouples. Model food samples were heated at 80 °C from 5 to 240 min (excluding CUT) and 100 °C from 5 to 150 min (excluding CUT) in triplicate. These time-temperature combinations were selected to be relevant to pasteurization with MAPS and conventional methods; longer heating times were needed to find the saturation of M-2 and color (Lau et al., 2003; Pandit et al., 2006). Model food samples for the three replicates of each time point came from three separate experimental batches. The results from this study at 80 and 100 °C were combined with findings from Bornhorst et al. (2017) at 90 °C to facilitate the determination of the temperature sensitivity of the chemical marker and color change of each model food.

Chemical marker, M-2 (4-hydroxy-5-methyl-3(2H)-furanone) concentration was quantified using high performance liquid chromatography (HPLC) with an adapted method from Bornhorst et al. (2017) and Zhang et al. (2014). Briefly, mashed potato samples were homogenized in 10 mmol/L H_2SO_4 extraction buffer, followed by centrifugation and filtration. An Agilent 1100 HPLC system (Agilent Technologies, Santa Clara, CA) was set up with a diode array detector and a 100 × 7.8 mm fast acid analysis column (Bio-Rad

Laboratories, Hercules, CA). Samples were analyzed using an injection volume of 25 μL with 10 mmol/L H_2SO_4 mobile phase at 1 mL/min with a detecting wavelength of 285 nm. All three experimental replicates for each time point were analyzed twice (2 analytical replicates) to determine M-2 concentration. Commercial M-2 (Sigma-Aldrich Co. LLC, St. Louis, MO) was utilized to generate standard curves, which were employed to determine the limit of detection and the M-2 concentration of an unknown mashed potato model food sample. The limit of detection was determined to be 0.02 mg M-2/L based on the ratio of 3 times the standard deviation of the response to the slope of the calibration curve, as described by [Shrivastava and Gupta \(2011\)](#).

Color was quantified in $L^*a^*b^*$ (CIELAB) color space using a computer vision system with hardware as described in [Pandit, Tang, Liu, and Mikhaylenko \(2007a\)](#) and camera settings and image analysis methods as described in [Bornhorst et al. \(2017\)](#). Briefly, hardware included a light pod, compact fluorescent light bulbs, a digital camera, and a computer with image acquisition software. Camera settings included a speed of 15 frames per second, ISO sensitivity of 200, and F (aperture value) of 11. Color correction and image analysis were performed using MATLAB R2013a. Color correction and conversion from RGB to $L^*a^*b^*$ utilized a color reference card (QPcard 203, QPcard AB, Helsingborg, Sweden) and a quadratic correction model adapted from [Leon, Mery, Pedreschi, and Leon \(2006\)](#). Image analysis for each sample included the application of a color correction and analysis of a circle containing 37,695 pixel values.

2.3. Kinetic data analysis

Based on the results from [Bornhorst et al. \(2017\)](#) and preliminary color data from this study, L^* and a^* values were utilized to represent color change and b^* values were disregarded due to insignificant Pearson correlation coefficients (<0.6) between b^* value and heating time. In order to determine the reaction kinetics for color (L^* and a^*) and M-2 concentration, a modified two-step non-linear regression method was utilized ([Lau et al., 2003](#)). The first step was to fit zero, first, and second order rate equations to the data using non-linear regression. For example, the first order equation was defined as ([Lau et al., 2003](#)):

$$C = C_{\infty} - (C_{\infty} - C_0)\exp(-kt) \quad (1)$$

where C is the value of the parameter (M-2, L^* , or a^*) at time t (min), C_{∞} is the value of the parameter at saturation (M-2 $_{\infty}$, L^*_{∞} , or a^*_{∞}), C_0 is the initial value of the parameter (M-2 $_0$, L^*_0 , or a^*_0), and k is the reaction rate constant (1/min). Eq. (1) was multiplied by -1 for L^* value because the L^* value decreased with increasing time. To determine the C_0 , C_{∞} , and k for each parameter (M-2, L^* , or a^*) at each temperature, the Newton algorithm for non-linear regression in SAS[®] 9.2 was employed. M-2 $_0$ was assigned to be a constant (zero) because experimental results showed the initial M-2 concentration was zero for all models. The kinetic model utilized in this study only considered the formation of M-2 and did not take into account any elimination reactions occurring simultaneously for this intermediate compound. This approach was selected based on the promising results in previous work for modeling Maillard reaction products in model foods ([Bornhorst et al., 2017](#); [Lau et al., 2003](#); [Pandit et al., 2006](#); [Wang et al., 2004](#)).

All three experimental replicates for each time point were input into the model to better reflect system variation compared to inputting average values. For each regression, the coefficient of determination (R^2) values were determined and utilized to identify which reaction order rate equation fit best. The second step was a standard linear regression using the Arrhenius equation to model

the impact of temperature change on the reaction rate constants. The Arrhenius relationship was determined using ([Toledo, 2007](#)):

$$k = A_0 \exp\left(-\frac{E_a}{RT}\right) \quad (2)$$

where k is the reaction rate (1/min) at temperature T (K), A_0 is the rate constant (1/min) as the temperature approaches infinity, E_a is the activation energy (kJ/mol), and R is the universal gas constant (0.008314 kJ/K/mol).

Thermal resistance of quality attributes can also be described by the decimal reduction time (D-value) and thermal resistance constant (z-value). D-value is the time (min) needed for a parameter (M-2, L^* , or a^*) to achieve a one log (90%) change at a given temperature; D-value was calculated from the reaction rate constant, as described in [Toledo \(2007\)](#). Z-value is the temperature change ($^{\circ}\text{C}$) needed to achieve a one log change in D-values; z-value was calculated from the activation energy, as described in [Toledo \(2007\)](#). The D and z-value approach to describe safety and quality attributes' change during thermal processing is very common. For this reason, D and z-values were reported to facilitate the use of reaction kinetic data from this study in future research.

The accumulated thermal lethality, F_{90} , was determined for *C. botulinum* using ([Toledo, 2007](#)):

$$F_{90} = \int_0^t 10^{(T-90)/z} dt \quad (3)$$

where F_{90} is the equivalent thermal treatment time (min) at 90°C , T is the temperature ($^{\circ}\text{C}$) at time t (min), and z is the thermal resistance constant with a value of 10°C for the pathogen mentioned above ([FDA, 2011](#); [ECFF, 2006](#)). Cook value (C_{100}) is commonly used as a food quality indicator; the accumulated cook value was calculated using ([Toledo, 2007](#)):

$$C_{100} = \int_0^t 10^{(T-100)/z} dt \quad (4)$$

where C_{100} is the equivalent thermal treatment time (min) at 100°C , T is the temperature ($^{\circ}\text{C}$) at time t (min), and z is the thermal resistance constant with a value of 33°C for overall food quality ([Toledo, 2007](#)). For both F_{90} and C_{100} calculations, the temperature was measured in the geometric center of the test cells (cold spot) throughout the heating time using calibrated type-T thermocouples. Thus, F_{90} and C_{100} reflected the minimum accumulated thermal lethality and cook value inside the test cell. Pearson correlation coefficients were calculated to test for correlation strength between thermal treatment severity (F_{90} and C_{100}) and color and M-2 concentration. SAS[®] 9.2 was employed for the analysis with a p-value for significance of less than 0.05.

2.4. Validation

Pasteurization validation studies were conducted in duplicate with 280 g trays of 1 g/100 g ribose, 1 g/100 g lysine mashed potato model food processed in both a microwave assisted pasteurization system (MAPS) and two types of conventional hot water methods (preheated and not preheated). Model food samples for the two replicates of each process came from two separate experimental batches. The MAPS design consisted of preheating the trays in warm water, microwave heating and holding in hot water, and cooling in water cold, all without overpressure. The hot water process utilized recirculating hot water baths with no overpressure

followed by cooling in cold water. Model food samples were placed in rigid, high barrier, polypropylene trays with an ethylene vinyl alcohol barrier layer (Printpack, Inc. Atlanta, GA) and a rectangular shape (161 mm length, 116 mm width, 32 mm depth); trays were sealed with flexible, plastic lid-stock (Printpack, Inc. Atlanta, GA) under 15 MPa of vacuum.

All three processes aimed to achieve a 6 log reduction at the cold spot for non-proteolytic *C. botulinum*, the target food pathogen in this study; this equated to a minimum thermal treatment of 90 °C for 10 min (FDA, 2011; ECFE, 2006). Initial tests were conducted to determine the cold spot in MAPS processed model food trays and the temperature was measured at the cold spot every 2 s using calibrated, mobile metallic sensors and data logging software (TMI, USA, Inc. Reston, VA), as described in Luan, Tang, Pedrow, Liu, and Tang (2013). The temperature was also measured every 2 s during both hot water processes at the cold spot, which was the geometric center of the tray. Several iterations for each process with varying heating and holding times were tested in order to achieve a process with sufficient thermal treatment. The final MAPS process included 30 min of preheating in 61 °C water, 2.3 min of microwave heating with trays in 93 °C water, 9 min of holding in 93 °C water, and 5 min of cooling in 23 °C water. The hot water process with preheating included 30 min of preheating in 61 °C water, 32.2 min of heating in 93 °C water and 10 min of cooling in 5 °C water. The hot water process without preheating included 38 min of heating in 93 °C water followed by 10 min of cooling in 5 °C water. The MAPS, hot water process with preheating, and hot water process without preheating yielded thermal treatment equivalents (F_{90}) at the cold spot of 90 °C for 10.9, 11.0, and 10.9 min, respectively.

After processing and cooling to room temperature (22 °C), the trays of model foods were sliced horizontally at $\frac{1}{4}$ and $\frac{1}{2}$ the sample thickness (quarter and middle layers). The color of the quarter and middle layers was analyzed using the computer vision system described above. During image analysis, color mapping was performed to visualize the heating pattern, where the L^* and a^* values in the images were transformed to a jet color scale in MATLAB R2013a. The L^* color map utilized an L^* value range of 20–68 and the a^* color map utilized an a^* value range of 1–22, based on the initial and saturation color data from the kinetic study. This approach to creating color maps based on L^* and a^* values was unique and differed from previous work that utilized grayscale values (Pandit et al., 2007a; Zhang et al., 2014). Statistical analysis was performed to generate histograms for the pixel values in each image; histogram data were normalized using the total number of pixels in each image.

3. Results and discussion

3.1. Quantification of chemical marker (M-2)

M-2 concentration increased with increasing time until apparent saturation concentration ($M-2_{\infty}$) was achieved (Fig. 1). As expected, mashed potato samples heated at 100 °C had higher M-2 concentrations compared to those heated at 80 °C. During the first 150 min, all three model food formulas heated at 100 °C achieved an apparent saturation of M-2 concentration, while the M-2 concentration in model food samples heated at 80 °C continued to increase throughout the heating time. For this reason, additional time points up to 240 min of heating were utilized for samples heated at 80 °C to better understand and model the M-2 concentration.

M-2 formation in mashed potato model foods heated at 80 and 100 °C fit first order kinetics best, with R^2 values above 0.99 for 1 g/100 g ribose, 0.5 g/100 g lysine, 0.97 for 1 g/100 g ribose, 1 g/100 g

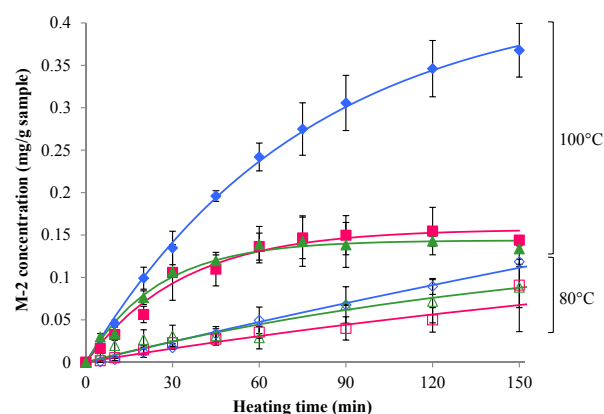


Fig. 1. Experimental chemical marker M-2 concentration (3 replicates) with 95% confidence intervals during heating with added precursor amounts of 1 g/100 g ribose and 0.5 g/100 g lysine (80 °C: \diamond , 100 °C: \blacklozenge), 1 g/100 g ribose and 1 g/100 g lysine (80 °C: \square , 100 °C: \blacksquare), and 2 g/100 g ribose and 2 g/100 g lysine (80 °C: \triangle , 100 °C: \blacktriangle). M-2 concentrations predicted with the first order kinetic model are also shown (—).

lysine, and 0.94 for 2 g/100 g ribose, 2 g/100 g lysine. This trend matched previous work on M-2 reaction kinetics; Bornhorst et al. (2017) concluded M-2 formation at 90 °C in mashed potato, gelatin, and egg white model foods followed first order reaction kinetics and M-2 formation at 116–131 °C in mashed potato (Pandit et al., 2006) and whey protein (Lau et al., 2003) also fit best to first order kinetics.

For all three formulas, the M-2 saturation values ($M-2_{\infty}$) were similar at differing temperatures (Table 1). However, at each temperature, $M-2_{\infty}$ decreased with increasing amounts of added precursors, which agreed with results from Pandit et al. (2006) and Bornhorst et al. (2017). Alternative Maillard reaction pathways that yield brown color without M-2 formation may be enhanced in model food systems with greater amounts of added precursors, as proposed by Bornhorst et al. (2017).

At each temperature, M-2 formation rates increased with increasing precursor amounts, ranging from 1.5 to 40.3×10^{-3} 1/min (D-values 57–1588 min) (Table 1). This trend matched expectations for a first order reaction with limited reactants. Bornhorst et al. (2017) and Pandit et al. (2006) suggested that the limiting factor for the M-2 formation reaction rate is amino acid content. It follows that mashed potato model foods in this study that contain greater amounts of added lysine would have a faster reaction rate. Mashed potato model food systems with greater levels of added precursors also had higher pH; samples with no added precursors had a measured pH of 5.2, which increased to 8.4 for the 1_R, 0.5_L formula, 9.2 for the 1_R, 1_L formula, and 9.5 for the 2_R, 2_L formula. In this pH range, higher pH could have contributed to the increased reaction rate in model foods with more precursors (Ajandouz & Puigserver, 1999; Ajandouz, Tchiakpe, Dalle Ore, Benajiba, & Puigserver, 2001). Additionally, lower water activity in sample formulas with more precursors could also have contribute to the increased Maillard reaction rate.

For each formula, the reaction rate increased with increasing temperature and fit well to the Arrhenius equation with R^2 values above 0.98 for all three formulas. All formulas showed similar sensitivity to change in temperature, with activation energies between 104.9 and 122.3 kJ/mol (z-values: 20.6–24.0 °C). Activation energies for M-2 found in this study (104.9–122.3 kJ/mol) were within the range of those found at sterilization temperatures (116–131 °C) in a whey protein model food, i.e. 64.0–122.3 kJ/mol (Lau et al., 2003), and were larger than those in a mashed potato model food, i.e. 81.4–96.1 kJ/mol (Pandit et al., 2006). M-2

Table 1
Predicted chemical marker M-2 concentration at saturation ($M-2_{\infty}$), reaction rate constant (k), decimal reduction time (D -value), activation energy (E_a), and thermal resistance constant (z -value) with estimated standard error (3 replicates) for mashed potato model food samples with added precursor amounts of 1 g/100 g ribose and 0.5 g/100 g lysine (1_R, 0.5_L), 1 g/100 g ribose and 1 g/100 g lysine (1_R, 1_L), and 2 g/100 g ribose and 2 g/100 g lysine (2_R, 2_L) heated at 80, 90, and 100 °C. 90 °C reaction rates were repeated from Bornhorst et al. (2017) for comparison to other temperatures.

Precursor amount	Temperature (°C)	$M-2_{\infty}$ (mg M-2/g sample)	k (10^{-3} 1/min)	D -value (min)	E_a (kJ/mol)	z -value (°C)
1_R, 0.5_L	80	0.57 ± 0.17	1.5 ± 0.5	1588 ± 558	121.1 ± 8.1	20.8 ± 1.4
	90 ^a	0.47 ± 0.06	5.1 ± 0.9	449 ± 81		
	100	0.43 ± 0.02	13.2 ± 1.1	174 ± 14		
1_R, 1_L	80	0.18 ± 0.08	3.2 ± 1.8	720 ± 404	122.3 ± 19.5	20.6 ± 3.4
	90 ^a	0.24 ± 0.03	7.4 ± 1.8	310 ± 74		
	100	0.16 ± 0.01	30.0 ± 3.7	77 ± 9		
2_R, 2_L	80	0.15 ± 0.03	6.0 ± 1.8	387 ± 116	104.9 ± 8.9	24.0 ± 2.0
	90 ^a	0.10 ± 0.01	18.3 ± 4.1	126 ± 28		
	100	0.14 ± 0.01	40.3 ± 3.7	57 ± 5		

^a Data at 90 °C from Bornhorst et al. (2017).

formation in this study was more sensitive to changes in temperature (larger E_a) than M-2 formation in Pandit et al. (2006); this could be attributed to the difference in model food formulas, as formulas in this study had greater amounts of added precursors (1–2 g/100 g ribose, 0.5–2 g/100 g lysine) compared to the formula (1.5 g/100 g ribose, 0 g/100 g lysine) used by Pandit et al. (2006). Model foods with greater temperature sensitivity developed in this study may be advantageous for modeling food quality degradation that occurs during pasteurization and degradation in foods with increased temperature sensitivity. This study cannot be compared to previous work at pasteurization temperatures on egg white model food by Zhang et al. (2014) because the activation energies (or z -values) were not reported.

3.2. Effect of experimental variables (time and temperature) on color change

All model foods showed increased brown color formation with increasing heating time until an apparent saturation was reached (Fig. 2). As expected, model foods with more added precursors (ribose and lysine) had more brown color formation; this brown color formation was faster at higher temperatures. Color formation (L^* and a^* values) in the 1 g/100 g ribose, 0.5 g/100 g lysine formula at 80 °C was too slow to be accurately captured in 240 min; with this slow reaction rate, longer times up to 360 min were added to determine the reaction kinetics.

Brown color formation during heating at 80 and 100 °C in mashed potato model foods, as measured by L^* value, fit best to first order kinetics, with R^2 values above 0.84 for 1_R, 0.5_L, 0.92 for 1_R, 1_L, and 0.95 for 2_R, 2_L. Color change, as measured by a^* value, also fit best to first order kinetics at 80 and 100 °C, with R^2 values above 0.91 for 1_R, 0.5_L, 0.93 for 1_R, 1_L, and 0.96 for 2_R, 2_L. First order reaction kinetics for color change in this study matched trends found by Bornhorst et al. (2017) for Maillard browning color formation in egg white, gellan, and mashed potato model foods at 90 °C. For the 1_R, 1_L formula, a^* reached saturation after heating for 60 min at 100 °C and data were restricted to up to 60 min for reaction kinetic analysis. For the 2_R, 2_L formula, L^* was restricted to 30 min of heating at 100 °C and a^* was restricted to 30 min of heating at 80 °C and 20 min of heating at 100 °C due to a rapid rate of color formation and short time to reach the apparent saturation.

At each temperature, color change reaction rates increased with increasing precursor amounts, ranging from 2.9 to 213.8×10^{-3} 1/min (D -values 11–805 min) for L^* value in Table 2 and 1.4 to 4747×10^{-3} 1/min (D -values 0.5–1657 min) for a^* value in Table 3. This trend was expected because color change was found to follow first order kinetics, and with limited reactants, the reaction rate

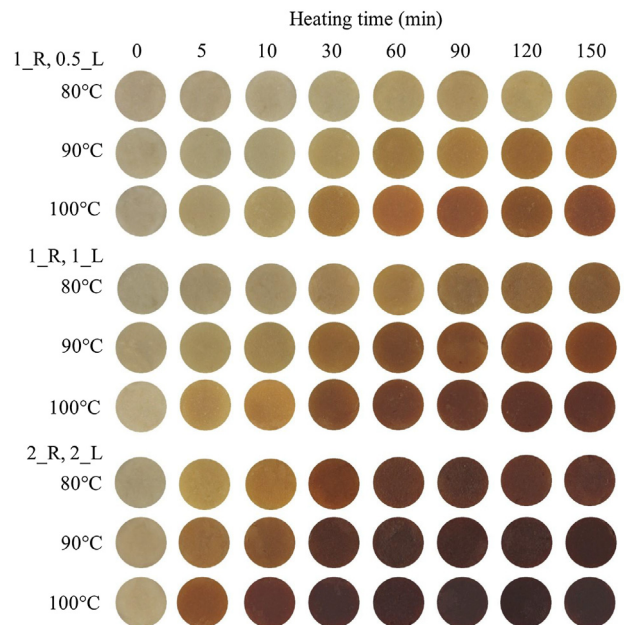


Fig. 2. Color change during heating at 80, 90, and 100 °C of mashed potato model food samples with added precursor amounts of 1 g/100 g ribose and 0.5 g/100 g lysine (1_R, 0.5_L), 1 g/100 g ribose and 1 g/100 g lysine (1_R, 1_L), and 2 g/100 g ribose and 2 g/100 g lysine (2_R, 2_L). 90 °C samples from Bornhorst et al. (2017) were added for comparison between temperatures.

should be higher when there are more reactants.

Similar to M-2 formation, L^* and a^* reaction rates increased with increasing temperature and fit well to the Arrhenius equation, with R^2 values above 0.92. The significant effect of temperature on L^* and a^* values was confirmed by Zhang (2014), who found significant correlation coefficients between both L^* and a^* values with temperature (60–90 °C) in solutions of water with added ribose and lysine. Activation energies for Maillard reaction brown color formation found by Kawai, Hagiwara, Takai, and Suzuki (2004) for glucose-lysine glassy model food matrices at 50–100 °C (130–156 kJ/mol) were within the range of those found in this study for color formation (87.7–245.6 kJ/mol). Differences between activation energies in this study and Kawai et al. (2004) could be attributed to differences in the type of sugar, water activity, and temperature range (van Boekel, 2001).

For all formulas, L^* value had a similar sensitivity to temperature change with activation energies between 87.7 and 121.1 kJ/mol (z -values: 20.8–28.8 °C). The range of z -values across all formulas for

Table 2

Predicted initial L^* value (L^*_0), L^* value at saturation (L^*_∞), reaction rate constant (k), decimal reduction time (D -value), activation energy (E_a), and thermal resistance constant (z -value) with estimated standard error (3 replicates) for mashed potato model food samples with added precursor amounts of 1 g/100 g ribose and 0.5 g/100 g lysine (1_R, 0.5_L), 1 g/100 g ribose and 1 g/100 g lysine (1_R, 1_L), and 2 g/100 g ribose and 2 g/100 g lysine (2_R, 2_L) heated at 80, 90, and 100 °C. 90 °C reaction rates were repeated from Bornhorst et al. (2017) for comparison to other temperatures.

Model	Temp. (°C)	L^*_0	L^*_∞	k (10^{-3} 1/min)	D -value (min)	E_a (kJ/mol)	z -value (°C)
1_R, 0.5_L	80	67.7 ± 0.6	46.0 ± 6.5	2.9 ± 1.3	805 ± 377	87.7 ± 4.8	28.8 ± 1.6
	90 ^a	68.2 ± 1.3	39.5 ± 13.1	6.0 ± 4.6	381 ± 274		
	100	69.1 ± 0.8	37.7 ± 2.3	14.2 ± 2.3	162 ± 26		
1_R, 1_L	80	63.6 ± 0.7	27.0 ± 6.9	4.6 ± 1.4	501 ± 151	121.1 ± 36.6	20.8 ± 6.9
	90 ^a	66.1 ± 1.0	35.4 ± 0.9	25.4 ± 2.9	91 ± 10		
	100	66.0 ± 1.6	33.1 ± 1.2	41.5 ± 6.3	55 ± 8		
2_R, 2_L	80	67.2 ± 1.5	25.6 ± 0.9	30.1 ± 2.8	76 ± 7	107.2 ± 10.9	23.5 ± 2.4
	90 ^a	62.5 ± 1.2	22.7 ± 0.5	69.3 ± 5.2	33 ± 2		
	100	64.5 ± 1.5	24.3 ± 1.1	213.8 ± 25.5	11 ± 1		

^a Data at 90 °C from Bornhorst et al. (2017).

Table 3

Predicted initial a^* value (a^*_0), a^* value at saturation (a^*_∞), reaction rate constant (k), decimal reduction time (D -value), activation energy (E_a), and thermal resistance constant (z -value) with estimated standard error (3 replicates) for mashed potato model food samples with added precursor amounts of 1 g/100 g ribose and 0.5 g/100 g lysine (1_R, 0.5_L), 1 g/100 g ribose and 1 g/100 g lysine (1_R, 1_L), and 2 g/100 g ribose and 2 g/100 g lysine (2_R, 2_L) heated at 80, 90, and 100 °C. 90 °C reaction rates were repeated from Bornhorst et al. (2017) for comparison to other temperatures.

Model	Temp. (°C)	a^*_0	a^*_∞	k (10^{-3} 1/min)	D -value (min)	E_a (kJ/mol)	z -value (°C)
1_R, 0.5_L	80	0.0 ± 0.4	37.0 ± 19.4	1.4 ± 0.9	1657 ± 1087	158.1 ± 3.6	16.0 ± 0.4
	90 ^a	1.7 ± 0.6	28.3 ± 5.3	6.5 ± 2.1	355 ± 115		
	100	0.0 ± 0.7	20.8 ± 0.8	24.9 ± 2.8	92 ± 10		
1_R, 1_L	80	1.6 ± 0.6	17.3 ± 0.9	12.9 ± 2.2	178 ± 30	98.5 ± 7.7	25.6 ± 2.0
	90 ^a	2.4 ± 0.6	20.7 ± 0.5	28.8 ± 3.0	80 ± 8		
	100	2.4 ± 0.9	20.9 ± 0.8	78.1 ± 12.4	29 ± 5		
2_R, 2_L	80	0.5 ± 0.9	27.9 ± 3.5	52.5 ± 13.4	44 ± 11	245.6 ± 72.1	10.3 ± 3.3
	90 ^a	2.7 ± 0.7	19.9 ± 1.0	169.9 ± 28.7	14 ± 2		
	100	3.0 ± 1.0	18.8 ± 0.6	4747 ± 1661	0.5 ± 0.2		

^a Data at 90 °C from Bornhorst et al. (2017).

L^* value (20.8–28.8 °C) was similar to M-2 (20.6–24.0 °C), indicating that both reactions had a similar sensitivity to temperature change. The temperature sensitivity of a^* value differed from L^* and M-2, with a^* activation energies ranging from 98.5 to 245.6 kJ/mol (z -values: 10.3–25.6 °C). For the 1_R, 0.5_L and 2_R, 2_L formulas, a^* z -values were smaller than the L^* and M-2 z -values, which indicated that a^* value was more sensitive to changes in temperature. Both L^* and a^* values could be useful in image analysis and heating pattern visualization using the computer vision system approach. The use of individual tri-stimulus color components (L^* and a^*) for heating pattern visualization is a unique contribution of this study and differs from past work which only utilized a combined grayscale color value for visualization (Pandit et al., 2007a; Zhang et al., 2014).

3.3. Thermal lethality and cook value correlations

As mentioned previously, the minimum thermal lethality (F_{90}) needed at the coldest spot in a food product is 10 min; this treatment yields a minimum 6 log reduction in the target food pathogen, non-proteolytic *C. botulinum* (FDA, 2011; ECFE, 2006). However, initial tests showed that the thermal treatment of the hot spot during pasteurization processes can be much greater. An initial correlation assessment between M-2, L^* , and a^* values and thermal lethality (F_{90}) and cook value (C_{100}) was conducted for F_{90} up to 100 min and C_{100} up to 60 min. The primary correlation analysis included data from 0 to 240 min at 80 °C for F_{90} and C_{100} , 0–90 min of heating at 90 °C for F_{90} and C_{100} (data from Bornhorst et al., 2017), 0–5 min at 100 °C for F_{90} , and 0–45 min at 100 °C for C_{100} . The model foods with strong correlations (Pearson correlation

coefficients >0.7) would likely have the most relevance for process evaluation. A secondary correlation analysis of the cook value was conducted by restricting the data to a maximum C_{100} of 20 min. A maximum cook value of 20 min was selected to be relevant for pasteurization because preliminary results during pilot-scale pasteurization tests showed a maximum 20 min cook value for the hot spot.

In all three formulas, M-2, L^* , and a^* values were significantly correlated to both F_{90} and C_{100} (p -value <0.001), except a^* value in the 2_R, 2_L formula (Table 4). M-2 was well correlated to cook value and moderately correlated to thermal lethality, with correlation coefficients ranging from 0.89 to 0.96 for C_{100} and 0.39–0.58 for F_{90} . These results implied that M-2 formation in the mashed

Table 4

Pearson correlation coefficients for thermal lethality (F_{90}) and cook value (C_{100}) with experimental chemical marker M-2 concentration, L^* value, and a^* value (3 replicates) during heating at 80–100 °C. Chemical marker and color data were included for F_{90} up to 100 min and C_{100} up to 60 min. Model food samples had added precursor amounts of 1 g/100 g ribose and 0.5 g/100 g lysine (1_R, 0.5_L), 1 g/100 g ribose and 1 g/100 g lysine (1_R, 1_L), and 2 g/100 g ribose and 2 g/100 g lysine (2_R, 2_L).

Thermal severity	Model	M-2	L^*	a^*
F_{90}	1_R, 0.5_L	0.58*	−0.46*	0.58*
	1_R, 1_L	0.46*	−0.54*	0.60*
	2_R, 2_L	0.39*	−0.53*	0.40
C_{100}	1_R, 0.5_L	0.96*	−0.61*	0.85*
	1_R, 1_L	0.89*	−0.90*	0.85*
	2_R, 2_L	0.90*	−0.71*	0.55

*shows significant p -value of <0.001.

potato models would be more applicable for food quality evaluation than safety evaluation during pasteurization processing.

L^* value was well correlated (0.71–0.90) to cook value for the 1_R, 1_L and 2_R, 2_L formulas, moderately correlated to cook value for the 1_R, 0.5_L formula (0.61), and moderately correlated (0.46–0.54) to thermal lethality. The moderate correlation to cook value for the lowest precursor formula was likely due to a slower rate of L^* change compared to the greater precursor amount formulas. Similar to M-2 correlation findings, these results implied that L^* value was a better indicator of food quality change than safety.

a^* value was well correlated (0.85) to cook value for the 1_R, 0.5_L and 1_R, 1_L formulas, moderately correlated (0.40–0.60) to thermal lethality for all formulas and the cook value for the 2_R, 2_L formula. The moderate correlation for the formula with the highest precursor amounts was likely due to a very rapid rate of a^* change that quickly reached saturation, compared to the formulas with less added precursors. Similar to M-2 and L^* value correlation findings, these results implied that a^* value was a better indicator of food quality change than safety.

Across all model foods, correlation analysis showed that M-2, L^* , and a^* values would be better indicators for food quality than safety. M-2, L^* , and a^* values were plotted against cook value in

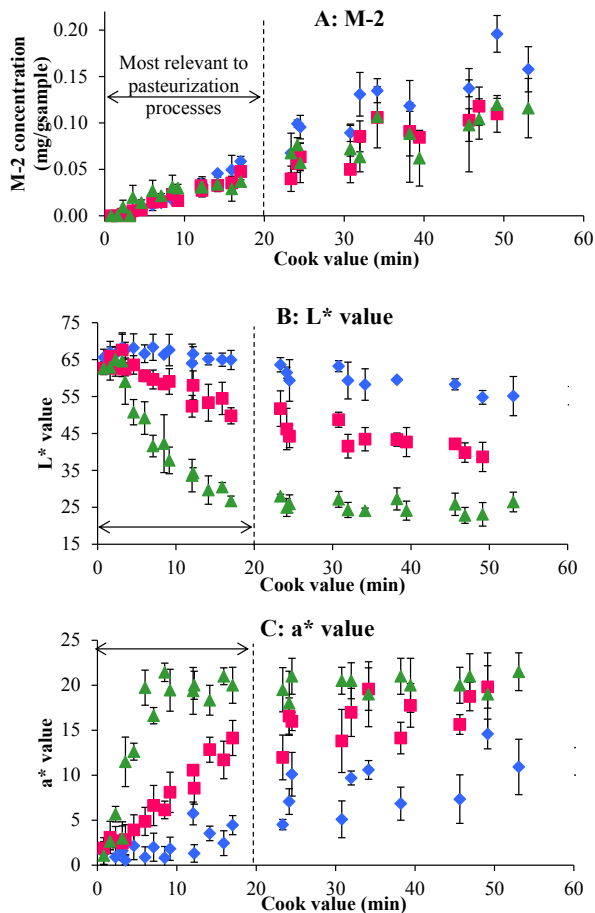


Fig. 3. Cook value (C_{100}) with experimental M-2 (A), L^* value (B) and a^* value (C) (3 replicates) during heating at 80–100 °C for model foods with 1 g/100 g ribose and 0.5 g/100 g lysine (◆), 1 g/100 g ribose and 1 g/100 g lysine (■), and 2 g/100 g ribose and 2 g/100 g lysine (▲). Cook values up to 20 min were most relevant to pasteurization process quality evaluation.

Fig. 3 to show a visual representation of the correlation. A secondary correlation analysis was conducted for a limited time range (C_{100} up to 20 min); as mentioned previously, this time range was selected to have more relevance to pasteurization process evaluation. When the cook value was restricted to up to 20 min, M-2 was well correlated to cook value for all formulas with significant correlation coefficients ranging from 0.79 to 0.96. When the cook value was restricted to up to 20 min for the color parameters, both L^* and a^* value were well correlated to cook value for the 1_R, 1_L and 2_R, 2_L formulas with significant correlation coefficients ranging from 0.84 to 0.88 for L^* value and 0.80–0.94 for a^* value. For the formula with the lowest precursor amounts (1_R, 0.5_L), both L^* and a^* values were weakly to moderately correlated to cook value with correlation coefficients ranging from 0.23 to 0.42. This trend can be explained by the slow rate of L^* and a^* value change in the lowest precursor formula during the first 20 min of cook value change. The secondary correlation analysis showed the model foods with strong, significant correlations to cook value were M-2 for all three formulas and L^* and a^* value for the 1_R, 1_L and 2_R, 2_L formulas (Fig. 3).

These findings were crucial in this study to show the applicability of mashed potato model foods for quantifying and evaluating food quality during pasteurization processes with varied time-temperature histories in the temperature range of 80–100 °C. The model food formulas with 1 g/100 g ribose, 1 g/100 g lysine and 2 g/100 g ribose, 2 g/100 g lysine had strong correlations between cook value and M-2, L^* value, and a^* value. The 1 g/100 g ribose, 1 g/100 g lysine formula was selected for use in the pasteurization validation tests because of these promising correlation results and less expensive cost due to the smaller amount of added precursors.

As mentioned above, correlation analysis results showed that the model food M-2 and color change during heating at pasteurization temperatures is more relevant for food quality evaluation than food safety. This finding differed from that of Bornhorst et al. (2017); they concluded that the models were equally good for both safety and quality evaluation at 90 °C. This difference could be explained by the study design, as the present study utilized various temperatures to simulate different time-temperature histories of a product, while Bornhorst et al. (2017) utilized only one temperature. When only one temperature is utilized, the model food reaction rate is the most important parameter in correlation analysis; when multiple temperatures and time-temperature histories are considered, the model food z-value becomes important. Model foods with strong correlation coefficients and the most relevance for process evaluation had reaction rates and z-values that were closer to those used in cook value calculations (z-value 33 °C) than in thermal lethality calculations (z-value 10 °C).

3.4. Model food validation using three pasteurization processes

Color change in 1 g/100 g ribose, 1 g/100 g lysine mashed potato model food was analyzed after pasteurizing 280 g trays using MAPS and hot water methods (Table 5). Results showed that model food trays pasteurized in the hot water processes had more color change in both middle and quarter layers than model food trays from MAPS. Among the hot water processed model foods, those that were not preheated had more color change compared to those that were preheated, especially in the quarter layer. Therefore, the hot water process with preheating was a less severe thermal treatment than the process without preheating; this demonstrated the potential value of using a preheating step for improving product quality.

Model food trays from both hot water processes had quarter layers with more a^* value color change than the middle layers,

implying that the model food closer to the outside of the package was overheated more than in the inside of the package. This result matched expectations based on conduction heat transfer theory; the outside of the package should receive more heat than the inside. In model food trays from MAPS, there were no significant color change differences between the middle and quarter layers. This demonstrated one of the potential advantages of using the MAPS process: the food product is less overheated, especially near the outside of the package.

Histograms for the middle layer L^* and a^* values were determined for the unheated control, MAPS, and hot water processed model food (Fig. 4). These results show that there was a color difference between the control, MAPS, and hot water processes and that this difference could be quantified using the image analysis techniques employed in this study. Both L^* and a^* value histograms show that the model food pasteurized in MAPS had less color change than both types of hot water processed model foods; the majority of color in the middle layer of the model food heated in MAPS had larger L^* values and smaller a^* values compared to hot water processed model foods. For model foods processed in hot water, those that were preheated had less color change (larger L^* values and smaller a^* values) compared to those that were not preheated.

Statistical analysis of the pixel data showed the interquartile range for L^* and a^* values were similar for all treatments, between 3 and 3.7 for L^* values and 1.4–2.4 for a^* values. This indicated that

the spread of the color data was similar among all treatments and showed the inherent variability in the color of the mashed potato model food. The median L^* values matched the trends described above, with the control having the greatest median L^* value of 75.7, followed by MAPS (63.5), hot water with preheating (59.5), and hot water without preheating (54.2). As expected, the opposite trend was found with a^* values, with the control having the smallest median a^* value of 1.7, followed by MAPS (10.2), hot water with preheating (14.2), and hot water without preheating (15.5). These results implied that the median was a more useful indicator of the overall color change severity, since the spread of the data were similar for all processes. The statistical analysis and histogram data confirmed the visual color change observations, as shown in Table 5.

Both the visual and quantitative image analysis results show that MAPS processed model food trays had less color change and a less severe thermal process, followed by the hot water with preheating and hot water without preheating. This finding matches expectations because the total time the trays of model food were submerged in 93 °C water was almost three times shorter for the MAPS process, with only 11.3 min in 93 °C water for MAPS, 32.2 min for the conventional, hot water process with preheating, and 38 min for the hot water process without preheating. These results implied that model foods pasteurized with MAPS may have had a better quality than the hot water processed model food trays. The promising validation results from this study indicate that these mashed potato model foods and image analysis techniques could be useful in evaluating and comparing the impact of various thermal pasteurization processes on food quality.

One potential application of the model food and image analysis techniques is in visualizing quality changes inside food products, volumetrically. Another future application is as quality evaluation tools to help optimize thermal processes to have the highest quality, while maintaining safety. For example, the model foods could be used to quantify food quality differences between processes: 85 °C for a longer time versus 90 °C or 95 °C for shorter times.

4. Conclusions

Chemical marker (M-2) and color formation (L^* and a^* values) in mashed potato model foods followed first order reaction kinetics, and temperature dependence followed an Arrhenius relationship. M-2 had the smallest range of reaction rates, followed by L^* value, and a^* value. Correlation analysis showed the model foods and parameters with strong, significant correlations were between M-2 and C_{100} for all three formulas, L^* value and C_{100} for the 1_R, 1_L and 2_R, 2_L formulas and a^* value and C_{100} for the 1_R, 0.5_L and 1_R, 1_L formulas. These findings were critical because they helped to justify the applicability of using mashed potato model foods in pasteurization process quality evaluation.

Pasteurization validation results demonstrated that there was a quantifiable color difference between model foods with different time-temperature histories, including the unheated control, microwave assisted thermal pasteurization system (MAPS), hot water with preheating, and hot water without preheating processes. Model foods pasteurized in the hot water processes had more color change than those from the MAPS process, implying that MAPS was a less severe thermal treatment. Mashed potato model foods and image analysis techniques from this study could be useful tools in the future for quality evaluation and optimization of MAPS and other thermal pasteurization methods.

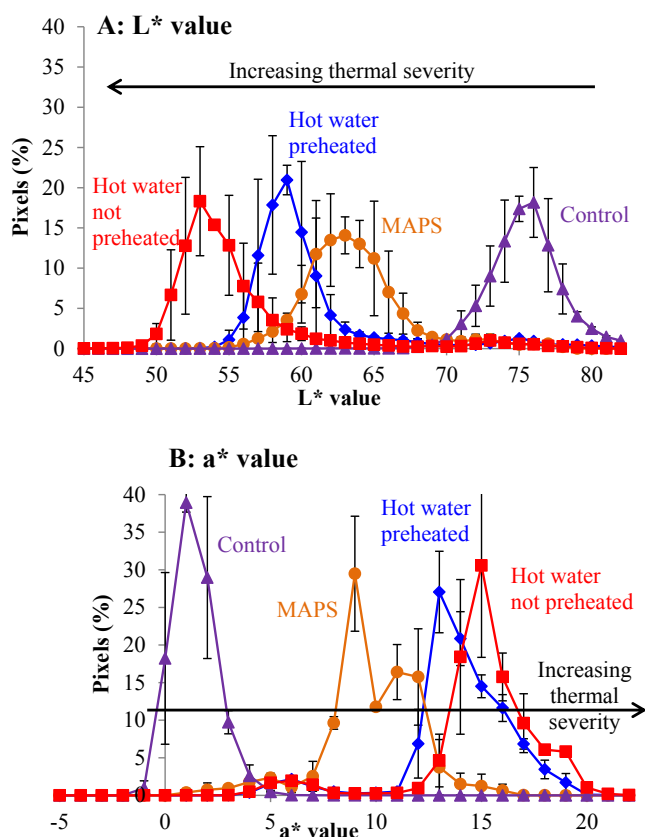


Fig. 4. Histograms of experimental, normalized pixel amounts (2 replicates) for L^* value (A) and a^* value (B) for the middle layer of 1 g/100 g ribose, 1 g/100 g lysine mashed potato model food trays of the control (unheated) sample (\blacktriangle), Microwave Assisted Pasteurization System (MAPS) processed (\bullet), and hot water processed with preheating (\blacklozenge) and without preheating (\blacksquare). The arrow shows the direction of increasing thermal severity and greater color change compared to the unheated control sample.

Table 5
Example images of 1 g/100 g ribose, 1 g/100 g lysine mashed potato model food trays after a conventional (hot water) pasteurization with and without preheating, Microwave Assisted Pasteurization System (MAPS), and an unheated control. For each tray, the middle and quarter layers are depicted by the original colored picture, L* value color map, and a* value color map.

Pasteurization process	Middle layer			Quarter layer		
	Original image	L* color map	a* color map	Original image	L* color map	a* color map
Hot water not preheated						
Hot water preheated						
MAPS						
Unheated control						

Acknowledgments

This research was supported in part by the National Institute of Food and Agriculture, U.S. Department of Agriculture (Agreement No. 2011-68003-20096 and 2016-68003-24840). Ellen Bornhorst's Ph.D. program at Washington State University was supported by the U.S. Department of Agriculture, National Needs Fellowship grant (2012-38420-19287).

References

- Ajandouz, E. H., & Puigserver, A. (1999). Nonenzymatic browning reaction of essential amino acids: Effect of pH on caramelization and Maillard reaction kinetics. *Journal of Agricultural and Food Chemistry*, 47, 1786–1793.
- Ajandouz, E. H., Tchiakpe, L. S., Dalle Ore, F., Benajiba, A., & Puigserver, A. (2001). Effects of pH on caramelization and Maillard reaction kinetics in fructose-lysine model systems. *Journal of Food Science*, 66, 926–931.
- BeMiller, J. N., & Huber, K. C. (2008). Carbohydrates. In S. Damodaran, K. L. Parkin, & O. R. Fennema (Eds.), *Fennema's food chemistry* (4th ed., pp. 83–154). Boca Raton, FL: CRC Press.
- Bornhorst, E. R., Tang, J., Sablani, S. S., & Barbosa-Cánovas, G. V. (2017). Development of model food systems for thermal pasteurization applications based on Maillard reaction products. *LWT-Food Science and Technology*, 75, 417–424.
- Chung, H. J., Birla, S. L., & Tang, J. (2008). Performance evaluation of aluminum test cell designed for determining the heat resistance of bacterial spores in foods. *LWT-Food Science and Technology*, 41, 1351–1359.
- European Chilled Food Federation (ECFF). (2006). *Recommendations for the production of prepackaged chilled food* (2nd ed.) <http://www.ecff.net/> Accessed 14.07.16.
- Fayle, S. E., & Gerrard, J. A. (2002). *The Maillard reaction*. Cambridge, UK: Royal Society of Chemistry.
- Food and Drug Administration (FDA). (2011). *Fish and fisheries products hazards and control guidance* (4th ed.). U.S. Department of Health and Human Services <https://www.fda.gov/>. Accessed 22.07.16.
- Kawai, K., Hagiwara, T., Takai, R., & Suzuki, T. (2004). Maillard Reaction rate in various glassy matrices. *Bioscience Biotechnology and Biochemistry*, 68, 2285–2288.
- Kim, H.-J., Taub, I. A., Choi, Y.-M., & Prakash, A. (1996). Principles and applications of chemical markers of sterility in high-temperature-short-time processing of particulate foods. In T. C. Lee, & H. J. Kim (Eds.), *Chemical markers for processed and stored foods* (pp. 54–69). Washington, D.C.: American Chemical Society.
- Kocadağı, T., & Gökmen, V. (2016). Effects of sodium chloride, potassium chloride, and calcium chloride on the formation of α -dicarbonyl compounds and furfurals and the development of browning in cookies during baking. *Journal of Agricultural and Food Chemistry*, 64, 7838–7848.
- Lau, M. H., Tang, J., Taub, I. A., Yang, T. C. S., Edwards, C. G., & Mao, R. (2003). Kinetics of chemical marker formation in whey protein gels for studying microwave sterilization. *Journal of Food Engineering*, 60, 397–405.
- Leon, K., Mery, D., Pedreschi, F., & Leon, J. (2006). Color measurement in L*a*b* units from RGB digital images. *Food Research International*, 39, 1084–1091.
- Luan, D., Tang, J., Pedrow, P. D., Liu, F., & Tang, Z. (2013). Using mobile metallic temperature sensors in continuous microwave assisted sterilization (MATS) systems. *Journal of Food Engineering*, 119, 552–560.
- Morris, E. R., Nishinari, K., & Rinaudo, M. (2012). Gelation of gellan—a review. *Food Hydrocolloids*, 28, 373–411.
- Pandit, R. B., Tang, J., Liu, F., & Mikhaylenko, G. (2007a). A computer vision method to locate cold spots in foods in microwave sterilization processes. *Pattern Recognition*, 40, 3667–3676.
- Pandit, R. B., Tang, J., Liu, F., & Pitts, M. (2007b). Development of a novel approach to determine heating pattern using computer vision and chemical marker (M-2) yield. *Journal of Food Engineering*, 78, 522–528.
- Pandit, R. B., Tang, J., Mikhaylenko, G., & Liu, F. (2006). Kinetics of chemical marker M-2 formation in mashed potato - a tool to locate cold spots under microwave sterilization. *Journal of Food Engineering*, 76, 353–361.
- Ramaswamy, H. S., Awuah, G. B., Kim, H. J., & Choi, Y. M. (1996). Evaluation of a chemical marker for process lethality measurement at 110C in a continuous flow holding tube. *Journal of Food Processing and Preservation*, 20, 235–249.
- Ross, E. W. (1993). Relation of bacterial destruction to chemical marker formation during processing by thermal pulses. *Journal of Food Process Engineering*, 16, 247–270.
- Shrivastava, A., & Gupta, V. B. (2011). Methods for the determination of limit of detection and limit of quantitation of the analytical methods. *Chronicles of Young Scientists*, 2, 21–25.
- Tang, J. (2015). Unlocking potentials of microwaves for food safety and quality. *Journal of Food Science*, 80, E1776–E1793.
- Tang, J., Tung, M. A., & Zeng, Y. (1996). Compression strength and deformation of gellan gels formed with mono- and divalent cations. *Carbohydrate Polymers*, 29, 11–16.
- Tang, J., Tung, M. A., & Zeng, Y. (1997). Gelling properties of gellan solutions containing monovalent and divalent cations. *Journal of Food Science*, 62, 688–692, 712.
- Toledo, R. T. (2007). *Fundamentals of food process engineering* (3rd ed.). New York: Springer (Chapters 8,9).
- van Boekel, M. (2001). Kinetic aspects of the Maillard reaction: A critical review. *Nahrung*, 45, 150–159.
- Van Loey, A., Hendrickx, M., De Cordt, S., Haentjens, T., & Tobback, P. (1996). Quantitative evaluation of thermal processes using time-temperature integrators. *Trends in Food Science & Technology*, 7, 16–26.
- Wang, Y., Lau, M. H., Tang, J., & Mao, R. (2004). Kinetics of chemical marker M-1 formation in whey protein gels for developing sterilization processes based on dielectric heating. *Journal of Food Engineering*, 64, 111–118.

- Wang, Y., Tang, J., Rasco, B., Wang, S. J., Alshami, A. A., & Kong, F. B. (2009). Using whey protein gel as a model food to study dielectric heating properties of salmon (*Oncorhynchus gorbuscha*) fillets. *LWT-Food Science and Technology*, *42*, 1174–1178.
- Wnorowski, A., & Yaylayan, V. A. (2002). Prediction of process lethality through measurement of Maillard-generated chemical markers. *Journal of Food Science*, *67*, 2149–2152.
- Zhang, W. (2014). *The development of time-temperature indicators for microwave assisted pasteurization processes*. PhD Thesis. Pullman, WA: Washington State University.
- Zhang, W. J., Luan, D. L., Tang, J. M., Sablani, S. S., Rasco, B., Lin, H. M., et al. (2015). Dielectric properties and other physical properties of low-acyl gellan gel as relevant to microwave assisted pasteurization process. *Journal of Food Engineering*, *149*, 195–203.
- Zhang, W., Tang, J., Liu, F., Bohnet, S., & Tang, Z. (2014). Chemical marker M2 (4-hydroxy-5-methyl-3(2H)-furanone) formation in egg white gel model for heating pattern determination of microwave-assisted pasteurization processing. *Journal of Food Engineering*, *125*, 69–76.